Transform-Limited Photon Emission from a Lead-Vacancy Center in Diamond above 10 K

Peng Wang,[1] Lev Kazak,[2] Katharina Senkalla,[2] Petr Siyushev,[2,3,4] Ryotaro Abe,[1] Takashi Taniguchi,[5] Shinobu Onoda,[6] Hiromitsu Kato,[7] Toshiharu Makino,[7] Mutsuko Hatano,[1] Fedor Jelezko,[2] and Takayuki Iwasaki[1,*]

[1]*Department of Electrical and Electronic Engineering, School of Engineering, Tokyo Institute of Technology, Meguro, 152-8552 Tokyo, Japan*
[2]*Institute for Quantum Optics, Ulm University, Albert-Einstein-Allee 11, D-89081 Ulm, Germany*
[3]*3rd Institute of Physics, University of Stuttgart, Pfaffenwaldring 57, 70569 Stuttgart, Germany*
[4]*Institute for Materials Research (IMO), Hasselt University, Wetenschapspark 1, B-3590 Diepenbeek, Belgium*
[5]*Research Center for Materials Nanoarchitectonics, National Institute for Materials Science, 305-0044 Tsukuba, Japan*
[6]*Takasaki Advanced Radiation Research Institute, National Institutes for Quantum Science and Technology, 1233 Watanuki, Takasaki, 370-1292 Gunma, Japan*
[7]*Advanced Power Electronics Research Center, National Institute of Advanced Industrial Science and Technology, Tsukuba, 305-8568 Ibaraki, Japan*

(Received 3 August 2023; accepted 22 December 2023; published 15 February 2024)

Transform-limited photon emission from quantum emitters is essential for high-fidelity entanglement generation. In this Letter, we report the coherent optical property of a single negatively charged lead-vacancy (PbV) center in diamond. Photoluminescence excitation measurements reveal stable fluorescence with a linewidth of 39 MHz at 6 K, close to the transform limit estimated from the lifetime measurement. We observe 4 orders of magnitude different linewidths of the two zero-phonon lines, and find that the phonon-induced relaxation in the ground state contributes to this huge difference in the linewidth. Because of the suppressed phonon absorption in the PbV center, we observe nearly transform-limited photon emission up to 16 K, demonstrating its high temperature robustness compared to other color centers in diamond.

DOI: 10.1103/PhysRevLett.132.073601

Color centers in diamond serve as prospective quantum repeaters in large-scale quantum networks [1–4], owing to their promising performance in the coherent manipulation of spin states [5,6] and efficient quantum light-matter interfaces [7,8]. Although two-photon interference [9] and quantum entanglement [3,10,11] based on the nitrogen-vacancy (NV) center have been reported thus far, the low fraction of emission into the zero-phonon line (ZPL) and instability due to large spectral diffusion pose a challenge for constructing a large-scale quantum network based on NV centers [12–14]. Alternatively, inversion-symmetric negatively charged group-IV vacancy centers, including silicon-vacancy (SiV), germanium-vacancy (GeV), tin-vacancy (SnV), and lead-vacancy centers (PbV), demonstrate large fluorescence concentrations in their ZPLs and high robustness against external noise [15,16]. In particular, the PbV center is predicted to exhibit a millisecond spin coherence time at 9 K [17], making it promising for quantum applications.

The Pb atom, comprising a PbV center, is the largest and heaviest among the stable group-IV elements, leading to severe lattice damage during ion implantation and difficulty in accommodating the Pb atom in the interstitial split-vacancy configuration in the diamond crystal; indeed, different ZPL wavelengths and large background emissions have been observed [18–21]. In our previous work [17], the high-temperature annealing over 2000 °C under high pressure has been applied for the formation of PbV centers, leading to the determination of the ZPL wavelengths. However, so far, the photon emission with the transform-limited linewidth determined by the excited-state radiative lifetime remains an open challenge, which is essential for high photon interference visibility in quantum networks [22,23]. Mitigation of phonon-induced relaxation and spectral diffusion plays an important role in achieving transform-limited photons. In this Letter, we investigate the optical properties of single PbV centers under resonant excitation and demonstrate that the C transition, one of the ZPLs, reaches the nearly transform limit at 6.2 K without prominent phonon-induced relaxation and spectral diffusion. On the other hand, the D transition, another ZPL, shows a linewidth 4 orders of magnitude broader than that of the C transition. We show that this stark contrast between the two ZPLs originates from phonon-induced relaxation in the ground state of the PbV center. Furthermore, the suppressed phonon relaxation on the C transition enables us to observe

the nearly transform-limited photons up to 16 K, in contrast to other group-IV vacancy centers in diamond.

The PbV centers are fabricated in a CVD-grown IIa-type diamond substrate. Ion implantation at an acceleration energy of 330 keV leads to a projected depth of 57 nm from the surface [17] according to SRIM calculations [24]. Subsequent high-pressure and high-temperature annealing (7.7 GPa, 2100 °C) leads to the formation of PbV centers and simultaneously recover the lattice damage generated during heavy-ion implantation [25,26]. The experiments are carried out on cryogenic home-built confocal microscope systems at varying temperatures. Photoluminescence (PL) measurements are carried out with a spectrometer with 532 nm laser excitation. Photoluminescence excitation (PLE) measurements are performed with a tunable dye laser and a wavemeter while measuring the phonon-sideband (PSB). The fluorescence detection for mapping and PLE are conducted based on the Qudi python module [27].

The PbV center in diamond possesses the same crystal and electronic structure as other group-IV vacancy centers; it contains an interstitial Pb atom and two neighboring vacancies, leading to D_{3d} symmetry with the main axis oriented along the $\langle 111 \rangle$ direction [17,28], as shown in Fig. 1(a). The large atomic size of Pb leads to poor accommodation in the diamond lattice, and thus, a rather severe strain environment is expected compared with other color centers [28]. The negatively charged PbV has 11 electrons, leading to a spin-1/2 system with a four-level energetic structure [Fig. 1(b)]. The spin-orbit interaction induces split ground ($\omega_{GS}/2\pi$) and excited ($\omega_{ES}/2\pi$) states, producing four ZPLs, labeled A, B, C, and D in the sequence of the energy decrease. The phonon absorption and emission between the sublevels in the ground state are depicted as dashed arrows, which will be discussed later. Figure 1(c) shows a PL spectrum at room temperature (~287 K) with 532 nm excitation. The prominent emissions at 552 nm and 556 nm correspond to the C and D transitions, respectively, followed by the PSB emission centered at 585 nm. The inset in Fig. 1(c) shows the fine structure of the emission, recorded at 6.2 K; the linewidth of the C transition is limited to the spectrometer resolution of ~50 GHz, while the D transition exhibits a much broader linewidth over 400 GHz. The ground state splitting is 3870 GHz estimated from the energy difference of the two peaks. According to the theoretical calculation [28], we estimate the Debye-Waller factor of PbV to be 0.34 at 6 K and 0.25 at room temperature, leading to a Huang-Rhys factor of 1.07 [29]. Although the Debye-Waller factor is lower than the other group-IV vacancy centers [26,40–42] due to the lattice distortion generated with the heavy atom in diamond [28], it is still about 10 times larger than that of the NV center in diamond [43,44]. The wavelengths of the A and B transitions predicted according to the excited state splitting (6920 GHz) from *ab initio* calculations [28] are indicated with blue arrows. They are not observed here due to insufficient thermal excitation into the upper branch in the excited state [17].

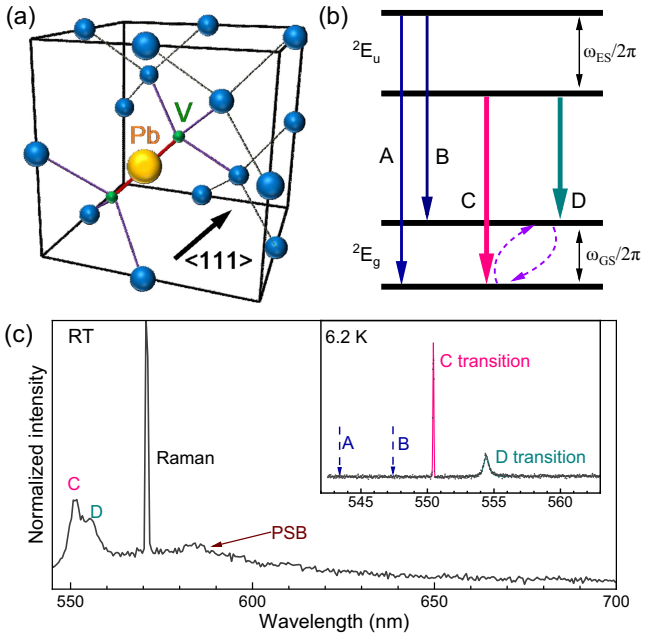

FIG. 1. Atomic structure and optical characteristics of the PbV center in diamond. (a) Crystal structure of the PbV center. (b) Four-level energetic structure of the PbV center and the corresponding optical transitions, labeled A, B, C, and D. The phonon-induced relaxation processes (phonon absorption and emission) in the ground states are shown by dashed arrows. (c) PL spectra of the PbV center at room temperature (RT) and 6.2 K (inset). The peaks at 550 nm (pink) and 554 nm (cyan) are the C and D transitions, respectively. The predicted A and B transitions are marked with blue arrows.

Then, we explore the coherent optical properties of a single PbV center in diamond. A time-resolved photoluminescence (TRPL) measurement is performed with a 532 nm pulsed laser. From the single exponential decay curve in Fig. 2(a), the radiative lifetime of the PbV center is estimated to be 4.4 ± 0.1 ns, leading to a transform-limited linewidth of 36.2 ± 0.8 MHz. A 550 nm bandpass filter used for TRPL enables the detection of both C and D transitions, and thereby, we assume that both have the same excited-state lifetime, as similar to SiV centers [45,46]. The PLE measurement is carried out by tuning the excitation laser, while detecting the PSB with a 561 nm longpass filter. Figure 2(b) shows a PLE spectrum of the C transition from the identical PbV center for the lifetime measurement above. The single-scan PLE spectrum under 1 nW resonant excitation demonstrates a narrow Lorentzian peak with a linewidth of 38.8 ± 0.3 MHz, which agrees with the transform-limited linewidth. Thus, the radiative transition plays a dominant role in the linewidth of the C transition of the PbV center at 6.2 K. The slight deviation from the transform-limited linewidth is possibly caused by power broadening and/or high-frequency spectral diffusion.

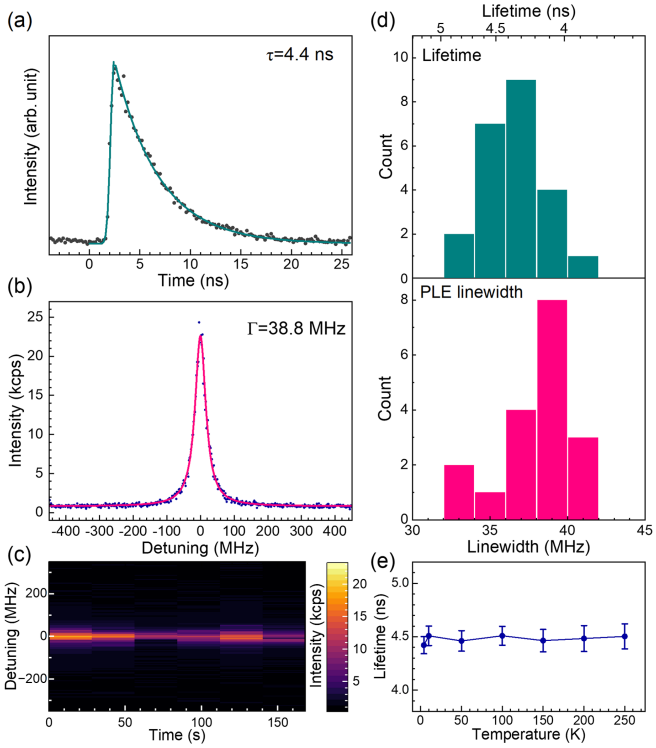

FIG. 2. Transform-limited emissions from PbV centers. (a) Time-resolved photon emission. (b) PLE spectrum of the C transition at 1 nW resonant excitation. (c) PLE spectra as a function of time. (d) Distribution of the radiative lifetime and single-scan PLE linewidth of multiple PbV centers. The top axis of the lifetime distribution is converted to the transform-limited linewidth (bottom axis). (e) Excited-state lifetime as a function of temperature.

During the repeated scans on the target single PbV center, no prominent peak shift is observed over time, as shown in Fig. 2(c). Averaging all PLE spectra yields a linewidth of 40.6 MHz, indicating that spectral diffusion is greatly suppressed in the PbV center formed by high-temperature annealing. Note that we occasionally observe a sudden termination of the emission close to zero detuning, as seen in the third and sixth scans of Fig. 2(c) and also Supplemental Material [29]. It is related to the charge conversion and has been reported in other group-IV vacancy centers [47–49]. A nonresonant 532 nm laser or even a resonant laser itself can serve as a repump laser to recover the emission [29]. Control of the charge state of the PbV center is of vital importance for future quantum applications.

The TRPL and PLE measurements are conducted on multiple PbV centers. Note that these two types of measurements are not performed for the same PbV centers. The distributions of the radiative lifetime and linewidth of the C transition are shown in Fig. 2(d). The mean lifetime of 4.4 ns corresponds to a transform-limited linewidth of 36 MHz, and matches the mean linewidth of 39 MHz obtained from the single-scan PLE measurements. Furthermore, the radiative lifetime of a PbV center at varying temperatures is measured. The lifetime is nearly constant from a cryogenic temperature to 250 K, as shown in Fig. 2(e). This is similar with the GeV center [50], and in contrast to the SiV center, which shows the decrease in the excited-state lifetime above 50–100 K [51,52]. The constant lifetime in the wide temperature range indicates a relatively high activation energy for nonradiative decay in the PbV center.

In contrast to the coherent C transition, another optical transition, the D transition shows significant broadening over 400 GHz even at low temperature in PL spectrum [inset in Fig. 1(c)]. Note that PLE spectrum of the D transition was not observed, which could be attributed to insufficient thermal excitation into the upper branch of the ground state and/or low intensity due to the broad linewidth. The large broadening of the D transition is completely different from the observation on the SiV center [45], where the two transitions exhibit similar narrow linewidths within 1.5 times the transform limit. For further comparison to another type of color center, we measure the PLE spectra of a GeV center [Fig. 3(a)]. The linewidths are 53.6 and 98.3 MHz for the C and D transitions, respectively, at 5 nW resonant excitation. A transform-limited linewidth of 28.9 MHz is obtained from the radiative lifetime [29], and a power broadening of 9.6 MHz is estimated from the C transition at 1 nW excitation [Fig. 3(a)]. Again, the slight broadening of the D transition on the GeV center does not match with the behavior of the PbV center.

To understand the measurement results, the relaxation processes in the group-IV vacancy centers are considered. The line broadening on a quantum emitter can be formulated as follows [22,53–55]:

$$\Gamma = \Gamma_0 + \Gamma_{\mathrm{ph}} + \Gamma_{\mathrm{others}}, \tag{1}$$

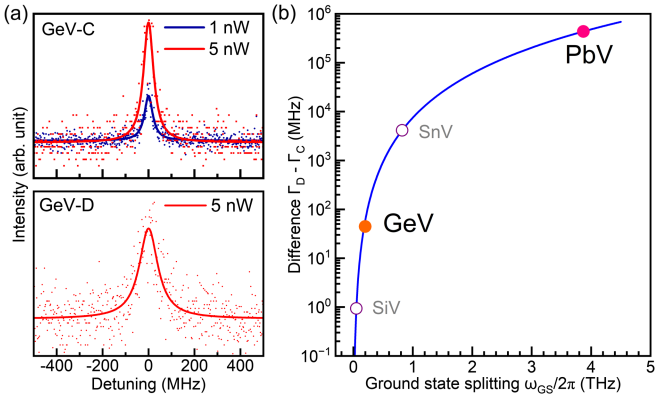

FIG. 3. Linewidth difference of the C and D transitions of group-IV vacancy centers in diamond. (a) PLE spectra of the C and D transitions of a GeV center at 6.2 K. (b) Linewidth difference between C and D transitions ($\Gamma_D - \Gamma_C$) as a function of the ground state splitting. The solid circle represents the experimental results of the GeV and PbV centers. The fitting is performed based on the phonon-induced relaxation model in Eq. (4) for GeV and PbV. The hollow circles are plotted according to the ground state splitting of the SiV and SnV centers.

where Γ_0 refers to the transform-limited linewidth directly obtained from the radiative lifetime, Γ_{ph} is the phonon-induced relaxation, and Γ_{others} comprises other effects such as power broadening and spectral diffusion. The power broadening is considered to be weak under low resonant power excitation. Additionally, a low nonresonant excitation power of 0.2 mW is used for PL of the D transition in Fig. 1(c), which is 1/9 of the saturation power [17]. Spectral diffusion does not play a significant role, as shown in Fig. 2(c). Conclusively, the broadening of the D transition in the PbV center is mainly attributed to the phonon-induced relaxation between the split energy levels.

The phonon-induced transition occurs in both the excited and ground states, where the latter is depicted in Fig. 1(b). In the ground state, phonon absorption and emission contribute to the line broadening of the C and D transitions, respectively. Because of the E-symmetry electronic structure in the group-IV vacancy center in diamond, only the electron-phonon coupling with the E-symmetric acoustic phonon modes can be considered [52,56]. We assume that single phonon processes, resonant to the split energies in the ground and excited states, are dominant at low temperatures. According to the Debye model and Fermi's golden rule, the phonon-induced transition rate is given as follows [29,52,53,57]:

$$\begin{cases} \gamma_s^+ = 2\pi\alpha\omega_s^3 n(\omega_s, T) \\ \gamma_s^- = 2\pi\alpha\omega_s^3 [n(\omega_s, T) + 1] \end{cases} \quad (s = \mathrm{GS}, \mathrm{ES}), \tag{2}$$

where γ_s^+ and γ_s^- represent the phonon absorption and emission rates, respectively, for a resonant phonon frequency of ω_s. GS and ES represent the ground state and excited state, respectively. $n(\omega_s, T)$ is the mean number of phonons at thermal equilibrium and defined as follows: $n(\omega_s, T) = [\exp(\hbar\omega_s/k_B T) - 1]^{-1}$, where k_B is the Boltzmann constant. α is a coupling parameter. Clearly, the phonon emission rate (γ_s^-) is larger than the phonon absorption rate (γ_s^+) for a given phonon frequency and temperature. Considering the electron-phonon interactions in both ground and excited states, Eqs. (1) and (2) lead to the linewidths of the C and D transitions as follows:

$$\begin{aligned} \Gamma_\mathrm{C} &= \Gamma_0 + \Gamma_{others} + \frac{1}{2\pi}(\gamma_\mathrm{GS}^+ + \gamma_\mathrm{ES}^+) \\ \Gamma_\mathrm{D} &= \Gamma_0 + \Gamma_{others} + \frac{1}{2\pi}(\gamma_\mathrm{GS}^- + \gamma_\mathrm{ES}^+). \end{aligned} \tag{3}$$

Importantly, the C transition is affected only by the phonon absorption in both the ground and excited states (γ_GS^+ and γ_ES^+), while the D transition contains the term on the phonon emission in the ground state (γ_GS^-). We obtain a relationship of the linewidth difference between the C and D transitions from Eqs. (2) and (3):

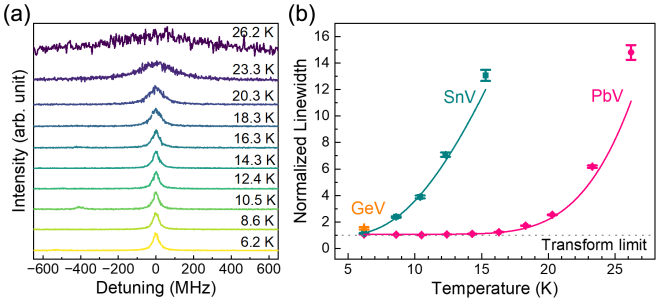

FIG. 4. Temperature dependence of the C transition. (a) PLE spectra of the C transition of the PbV center recorded at temperatures from 6.2 to 26.2 K. All spectra are obtained from three repeated scans. The peak centers are aligned for clarity. (b) Temperature-dependent linewidth of the C transition of group-IV vacancy centers in diamond. The linewidths are normalized to each transform limit (28.9 MHz for GeV, 30.6 MHz for SnV [58], and 36.2 MHz for PbV). The solid lines represent the calculations based on the phonon-induced relaxation model with the parameter α obtained in Fig. 3(b) and fitting parameters of $\Gamma_{others}(\mathrm{PbV}) = 2.7$ MHz and $\Gamma_{others}(\mathrm{SnV}) = -1.8$ MHz. The negative value for SnV is attributed to a possibly longer radiative lifetime of the target SnV compared to that of the ensemble state [58].

$$\Gamma_\mathrm{D} - \Gamma_\mathrm{C} = \frac{1}{2\pi}(\gamma_\mathrm{GS}^- - \gamma_\mathrm{GS}^+) = \alpha\omega_\mathrm{GS}^3. \tag{4}$$

This equation clearly indicates that the D transition is broader than the C transition independent of temperature. The difference in the linewidth depends on the ground state splitting, which increases as increasing the size of the group-IV element due to the stronger spin-orbit interaction [16].

The experimental linewidth differences of the GeV and PbV centers are well fitted with this cubic trend on the ground state splitting [Fig. 3(b)], with the coefficient α of $(2\pi)^{-3} \times 7.51 \times 10^{-9}$ GHz^{-2}. Therefore, the phonon-induced relaxation model above can explain the large broadening of the D transition in the PbV center. Note that the effect of the relaxation in the excited state (γ_ES^+) is rather small due to the large spin-orbit interaction [29]. Notably, according to the phonon relaxation model in this study, the SiV center has a very small linewidth difference below 1 MHz [Fig. 3(b)], which is challenging to experimentally observe. Moreover, the D transition of SnV with the predicted broad linewidth of approximately 5 GHz is not observed in our PLE measurements.

Finally, we discuss the temperature dependence of the coherent optical properties of the group-IV vacancy centers in diamond based on phonon-induced relaxation. Figure 4(a) shows the PLE spectra of the C transition of the PbV center at different temperatures. The linewidths are summarized in Fig. 4(b), together with the data of the GeV center from Fig. 3(a) and a SnV center [29] for comparison. Note that the linewidths are normalized to the transform-limited linewidth for each color center: 28.9 MHz for

GeV [29], 30.6 MHz for SnV [58], and 36.2 MHz for the PbV center. Surprisingly, the nearly transform-limited photon from the PbV center is observed above 10 K, indicating the weak phonon-induced relaxation of the C transition even at elevated temperatures. The solid lines represent the linewidths of the C transition of the SnV and PbV centers calculated by Eq. (3) with a fitting parameter Γ_{others}, assuming a negligible contribution of phonon relaxation in the excited state [29]. The calculated values agree with the experimental observations below 20 K. The discrepancy at higher temperatures could be attributed to second-order electron-phonon interactions [52], leading to a cubic temperature dependence of the emission linewidth [17], which has been also observed in other group-IV vacancy centers in diamond [26,46,52,59].

Line broadening beyond the transform-limit causes indistinguishability degradation in two-photon interference. With an emission linewidth of approximately 1.2 times the transform limit, a visibility of ∼80% is obtained for two-photon interference [22]. To satisfy this condition, according to the phonon-induced relaxation model, the SiV and GeV centers require cooling to 4–5 K, while the temperature tolerance of the SnV center is 6 K. In contrast, the estimated temperature for the PbV center reaches 16 K, which agrees with the experimental observation [Fig. 4(b)]. This temperature is also higher than an estimated temperature of ∼11 K for the NV center in diamond [60,61]. This superior thermal characteristic opens great opportunity to build energy-efficient scalable quantum networks based on the PbV center in diamond.

In conclusion, we obtained transform-limited photon emission without evident spectral diffusion from the C transition of a single PbV center in diamond. The coherent optical transitions for multiple PbV centers were confirmed. The large difference in the linewidth on the C and D transitions are well explained by considering the phonon-induced relaxation. With the experimental results of the GeV and PbV centers, we derive an electron-phonon interaction coupling parameter (α). The temperature dependence of the linewidth of the C transition was explained using this α value for the SnV and PbV centers. Owing to its large ground state splitting, the PbV center displayed high-temperature robustness of the coherent optical property up to 16 K, much higher than those for other group-IV vacancy centers in diamond. These results pave the way for the PbV center to become building blocks to construct large-scale quantum networks.

The authors would like to thank Masahiko Ogura, Tuan Minh Hoang, and Kohei Suda for support in the sample preparation, and Yasuyuki Narita, Kazuki Oba, and Yoshiyuki Miyamoto for fruitful discussions. This work is supported by JSPS KAKENHI (Grants No. JP22H04962, No. JP22H00210, and No. JP23KJ0931), the Toray Science Foundation, the MEXT Quantum Leap Flagship Program (Grant No. JPMXS0118067395), and JST Moonshot R&D (Grant No. JPMJMS2062). F. J. acknowledges support of DFG via projects 386028944, 445243414, 387073854, BMBF via project SPINNING, CoGeQ and QR.X, ERC via Synergy Grant HyperQ.

*Corresponding author: iwasaki.t.aj@m.titech.ac.jp

[1] A. Sipahigil *et al.*, An integrated diamond nanophotonics platform for quantum-optical networks, Science **354**, 847 (2016).
[2] C. T. Nguyen *et al.*, Quantum network nodes based on diamond qubits with an efficient nanophotonic interface, Phys. Rev. Lett. **123**, 183602 (2019).
[3] M. Pompili *et al.*, Realization of a multinode quantum network of remote solid-state qubits, Science **372**, 259 (2021).
[4] M. Ruf, N. H. Wan, H. Choi, D. Englund, and R. Hanson, Quantum networks based on color centers in diamond, J. Appl. Phys. **130**, 070901 (2021).
[5] N. Bar-Gill, L. M. Pham, A. Jarmola, D. Budker, and R. L. Walsworth, Solid-state electronic spin coherence time approaching one second, Nat. Commun. **4**, 1743 (2013).
[6] D. D. Sukachev, A. Sipahigil, C. T. Nguyen, M. K. Bhaskar, R. E. Evans, F. Jelezko, and M. D. Lukin, Silicon-vacancy spin qubit in diamond: A quantum memory exceeding 10 Ms with single-shot state readout, Phys. Rev. Lett. **119**, 223602 (2017).
[7] B. B. Zhou, P. C. Jerger, V. O. Shkolnikov, F. J. Heremans, G. Burkard, and D. D. Awschalom, Holonomic quantum control by coherent optical excitation in diamond, Phys. Rev. Lett. **119**, 140503 (2017).
[8] C. Weinzetl, J. Görlitz, J. N. Becker, I. A. Walmsley, E. Poem, J. Nunn, and C. Becher, Coherent Control and wave mixing in an ensemble of silicon-vacancy centers in diamond, Phys. Rev. Lett. **122**, 063601 (2019).
[9] H. Bernien, L. Childress, L. Robledo, M. Markham, D. Twitchen, and R. Hanson, Two-photon quantum interference from separate nitrogen vacancy centers in diamond, Phys. Rev. Lett. **108**, 043604 (2012).
[10] B. Hensen *et al.*, Loophole-free bell inequality violation using electron spins separated by 1.3 kilometres, Nature (London) **526**, 682 (2015).
[11] H. Bernien *et al.*, Heralded entanglement between solid-state qubits separated by three metres, Nature (London) **497**, 86 (2013).
[12] A. Faraon, C. Santori, Z. Huang, V. M. Acosta, and R. G. Beausoleil, Coupling of nitrogen-vacancy centers to photonic crystal cavities in monocrystalline diamond, Phys. Rev. Lett. **109**, 033604 (2012).
[13] P. Siyushev, H. Pinto, M. Vörös, A. Gali, F. Jelezko, and J. Wrachtrup, Optically controlled switching of the charge state of a single nitrogen-vacancy center in diamond at cryogenic temperatures, Phys. Rev. Lett. **110**, 167402 (2013).
[14] M. Leifgen *et al.*, Evaluation of nitrogen- and silicon-vacancy defect centres as single photon sources in quantum key distribution, New J. Phys. **16**, 023021 (2014).

[15] C. Bradac, W. Gao, J. Forneris, M. E. Trusheim, and I. Aharonovich, Quantum nanophotonics with group IV defects in diamond, Nat. Commun. **10**, 5625 (2019).
[16] T. Iwasaki, Color centers based on heavy group-IV elements, *in Semiconductors, and Semimetals*, edited by C. E. Nebel, I. Aharonovich, N. Mizuochi, and M. Hatano (Academic Press Inc., New York, 2020), Vol. 103, pp. 237–256, 10.1016/bs.semsem.2020.03.007.
[17] P. Wang, T. Taniguchi, Y. Miyamoto, M. Hatano, and T. Iwasaki, Low-temperature spectroscopic investigation of lead-vacancy centers in diamond fabricated by high-pressure and high-temperature treatment, ACS Photonics **8**, 2947 (2021).
[18] S. Ditalia Tchernij *et al.*, Single-photon emitters in lead-implanted single-crystal diamond, ACS Photonics **5**, 4864 (2018).
[19] M. E. Trusheim *et al.*, Lead-related quantum emitters in diamond, Phys. Rev. B **99**, 075430 (2019).
[20] J. E. Fröch *et al.*, Versatile direct-writing of dopants in a solid state host through recoil implantation, Nat. Commun. **11**, 5039 (2020).
[21] S. Ditalia Tchernij *et al.*, Spectral features of pb-related color centers in diamond—a systematic photoluminescence characterization, New J. Phys. **23**, 063032 (2021).
[22] B. Kambs and C. Becher, Limitations on the indistinguishability of photons from remote solid state sources, New J. Phys. **20**, 115003 (2018).
[23] C. Dangel, J. Schmitt, A. J. Bennett, K. Müller, and J. J. Finley, Two-photon interference of single photons from dissimilar sources, Phys. Rev. Appl. **18**, 054005 (2022).
[24] J. F. Ziegler, M. D. Ziegler, and J. P. Biersack, SRIM—The stopping and range of ions in matter (2010), Nucl. Instrum. Methods Phys. Res., Sect. B **268**, 1818 (2010).
[25] T. Iwasaki, Y. Miyamoto, T. Taniguchi, P. Siyushev, M. H. Metsch, F. Jelezko, and M. Hatano, Tin-vacancy quantum emitters in diamond, Phys. Rev. Lett. **119**, 253601 (2017).
[26] J. Görlitz *et al.*, Spectroscopic investigations of negatively charged tin-vacancy centres in diamond, New J. Phys. **22**, 013048 (2020).
[27] J. M. Binder *et al.*, Qudi: A modular PYTHON suite for experiment control and data processing, SoftwareX **6**, 85 (2017).
[28] G. Thiering and A. Gali, *Ab initio* magneto-optical spectrum of group-IV vacancy color centers in diamond, Phys. Rev. X **8**, 021063 (2018).
[29] See Supplemental Material at http://link.aps.org/supplemental/10.1103/PhysRevLett.132.073601 for details on single configuration, Debye-Waller factor,charge state conversion, fabrication and measurements on the GeV and SnV centers, phonon-induced relaxation, which includes Refs. [30–39].
[30] R. H. Brown, Richard Q. Twiss, and R. Q. Twiss, Correlation between photons in two coherent beams of light, Nature (London) **177**, 27 (1956).
[31] R. Brouri, A. Beveratos, J. P. Poizat, and P. Grangier, Photon antibunching in the fluorescence of individual color centers in diamond, Opt. Lett. **25**, 1294 (2000).
[32] T. Iwasaki *et al.*, Germanium-vacancy single color centers in diamond, Sci. Rep. **5**, 12882 (2015).
[33] D. Chen *et al.*, Quantum interference of resonance fluorescence from germanium-vacancy color centers in diamond, Nano Lett. **22**, 6306 (2022).
[34] A. Norambuena, A. Jimenez, C. Becher, and J. R. Maze, Effect of phonons on the electron spin resonance absorption spectrum, New J. Phys. **22**, 073068 (2020).
[35] W. Ulrich, *Quantum Dissipative Systems* 3rd Edition (World Scientific Publishing, Singapore, 2008), 10.1142/6738.
[36] A. Norambuena, E. Muñoz, H. T. Dinani, A. Jarmola, P. Maletinsky, D. Budker, and J. R. Maze, Spin-lattice relaxation of individual solid-state spins, Phys. Rev. B **97**, 094304 (2018).
[37] P. Udvarhelyi *et al.*, Vibronic states and their effect on the temperature and strain dependence of silicon-vacancy qubits in 4H-Si C, Phys. Rev. Appl. **13**, 054017 (2020).
[38] C. Hepp *et al.*, Electronic structure of the silicon vacancy color center in diamond, Phys. Rev. Lett. **112**, 036405 (2014).
[39] E. A. Ekimov, S. G. Lyapin, K. N. Boldyrev, M. V. Kondrin, R. Khmelnitskiy, V. A. Gavva, T. V. Kotereva, and M. N. Popova, Germanium–vacancy color center in isotopically enriched diamonds synthesized at high pressures, JETP Lett. **102**, 701 (2015).
[40] A. T. Collins, L. Allers, C. J. H. Wort, and G. A. Scarsbrook, The annealing of radiation damage in De Beers colourless CVD diamond, Diamond Relat. Mater. **3**, 932 (1994).
[41] O. Access, E. Neu, D. Steinmetz, J. Riedrich-Möller, S. Gsell, M. Fischer, M. Schreck, and C. Becher, Single photon emission from silicon-vacancy colour centres in chemical vapour deposition nano-diamonds on iridium, New J. Phys. **13**, 025012 (2011).
[42] Y. N. Palyanov, I. N. Kupriyanov, Y. M. Borzdov, and N. V. Surovtsev, Germanium: A new catalyst for diamond synthesis and a new optically active impurity in diamond, Sci. Rep. **5**, 14789 (2015).
[43] C. Santori, P. E. Barclay, K. M. C. Fu, R. G. Beausoleil, S. Spillane, and M. Fisch, Nanophotonics for quantum optics using nitrogen-vacancy centers in diamond, Nanotechnology **21**, 274008 (2010).
[44] G. Thiering and A. Gali, *Ab initio* calculation of spin-orbit coupling for an NV center in diamond exhibiting dynamic Jahn-Teller effect, Phys. Rev. B **96**, 081115(R) (2017).
[45] L. J. Rogers *et al.*, Multiple intrinsically identical single-photon emitters in the solid state, Nat. Commun. **5**, 4739 (2014).
[46] C. Arend, J. N. Becker, H. Sternschulte, D. Steinmüller-Nethl, and C. Becher, Photoluminescence excitation and spectral hole burning spectroscopy of silicon vacancy centers in diamond, Phys. Rev. B **94**, 045203 (2016).
[47] U. Jantzen *et al.*, Nanodiamonds carrying silicon-vacancy quantum emitters with almost lifetime-limited linewidths, New J. Phys. **18**, 073036 (2016).
[48] D. Chen, Z. Mu, Y. Zhou, J. E. Fröch, A. Rasmit, C. Diederichs, N. Zheludev, I. Aharonovich, and W. B. Gao, Optical gating of resonance fluorescence from a single germanium vacancy color center in diamond, Phys. Rev. Lett. **123**, 033602 (2019).
[49] J. Görlitz *et al.*, Coherence of a charge stabilised tin-vacancy spin in diamond, npj Quantum Inf. **8**, 45 (2022).

[50] M. K. Bhaskar *et al.*, Quantum nonlinear optics with a germanium-vacancy color center in a nanoscale diamond waveguide, Phys. Rev. Lett. **118**, 223603 (2017).
[51] F. Trojánek, K. Hamráček, M. Hanák, M. Varga, A. Kromka, O. Babčenko, L. Ondič, and P. Malý, Light emission dynamics of silicon vacancy centers in a polycrystalline diamond thin film, Nanoscale **15**, 2734 (2023).
[52] K. D. Jahnke, A. Sipahigil, J. M. Binder, M. W. Doherty, M. Metsch, L. J. Rogers, N. B. Manson, M. D. Lukin, and F. Jelezko, Electron-phonon processes of the silicon-vacancy centre in diamond, New J. Phys. **17**, 043011 (2015).
[53] I. S. Osad'ko, Determination of electron-phonon coupling from structured optical spectra of impurity centers, Sov. Phys. Usp. **22**, 311 (1979).
[54] R. Kubo, A stochastic theory of line shape, in *Advances in Chemical Physics* (John Wiley & Sons, Ltd., New York, 1969), Vol. 15, pp. 101–127, 10.1002/9780470143605.ch6.
[55] N. Morioka *et al.*, Spin-controlled generation of indistinguishable and distinguishable photons from silicon vacancy centres in silicon carbide, Nat. Commun. **11**, 2516 (2020).
[56] M. W. Doherty, N. B. Manson, P. Delaney, and L. C. L. Hollenberg, The negatively charged nitrogen-vacancy centre in diamond: The electronic solution, New J. Phys. **13**, 025019 (2011).
[57] V. Hizhnyakov, V. Boltrushko, H. Kaasik, and I. Sildos, Phase relaxation in the vicinity of the dynamic instability: Anomalous temperature dependence of zero-phonon line, J. Lumin. **107**, 351 (2004).
[58] Y. Narita, P. Wang, K. Ikeda, K. Oba, Y. Miyamoto, T. Taniguchi, S. Onoda, M. Hatano, and T. Iwasaki, Multiple tin-vacancy centers in diamond with nearly identical photon frequency and linewidth, Phys. Rev. Appl. **19**, 024061 (2023).
[59] Y. Chen, S. White, E. A. Ekimov, C. Bradac, M. Toth, I. Aharonovich, and T. T. Tran, Ultralow-power cryogenic thermometry based on optical-transition broadening of a two-level system in diamond, ACS Photonics **10**, 2481 (2023).
[60] Kai-Mei C. Fu, C. Santori, P. E. Barclay, L. J. Rogers, N. B. Manson, and R. G. Beausoleil, Observation of the dynamic Jahn-Teller effect in the excited states of nitrogen-vacancy centers in diamond, Phys. Rev. Lett. **103**, 256404 (2009).
[61] I. Aharonovich, S. Castelletto, D. A. Simpson, C. H. Su, A. D. Greentree, and S. Prawer, Diamond-based single-photon emitters, Rep. Prog. Phys. **74**, 076501 (2011).